Desalination and Water Treatment
www.deswater.com

doi: 10.5004/dwt.2018.22006

112 (2018) 207–217
April

Humic acid covered alumina as adsorbent for the removal of organic dye from coloured effluents

R. Ait Akbour[a], H. Ouachtak[a], A. Jada[b,*], S. Akhouairi[a], A. Ait Addi[a], J. Douch[a], M. Hamdani[a]

[a]*Laboratoire d'Électrochimie & Catalyse et Environnement, Faculté des Sciences d'Agadir, Université Ibn Zohr, Agadir, Morocco, emails: ak04rach@hotmail.fr (R. Ait Akbour), ouachtakhassan@gmail.com (H. Ouachtak), akhouairisiham@gmail.com (S. Akhouairi), a_aitaddi@yahoo.fr (A. Ait Addi), douch.791955@gmail.com (J. Douch), hamdani.mohamed@gmail.com (M. Hamdani)*
[b]*IS2M, CNRS-UHA, 15 Rue Jean Starcky, 68057 Mulhouse cedex, France, email: amane.jada@uha.fr*

Received 8 November 2017; 7 February 2018

ABSTRACT

In the present study, the potential use of humic acid (HA) covered alumina (ALHUM) as alternative and novel adsorbent material for the removal of methylene blue (MB) a basic dye, from aqueous solution within a batch process, was investigated. The covering efficiency was assessed by comparing the surface chemistry, the surface charge and the microstructure, of the natural and the HA covered alumina samples, and by using various tools such as streaming induced potential measurements and scanning electron microscopic analysis. The data indicate that increasing the coverage of the alumina support by HA, leads to enhancement of the dye removal from water. Such cationic dye removal from water was also found to increase by increasing either the aqueous phase pH or the temperature of the adsorption medium. However, decreases in the MB adsorbed amount were observed upon the increase of the divalent cation (Ca^{2+}, Ba^{2+} and Cu^{2+}) affinity toward the ALHUM and/or the aqueous solution ionic strength. These features highlight the suitability of ALHUM adsorbent for the treatment of water polluted with organic dyes. Three adsorption kinetic models (pseudo-first-order, pseudo-second-order and intra-particle diffusion) were used to fit the experimental kinetic data. The kinetic of MB adsorption was found to follow pseudo-first-order model. In addition, the adsorption data at the equilibrium were fitted to various theoretical predictions, and good agreements were found with the Dubinin–Radushkevich isotherm models, as compared with, the Langmuir and the Freundlich theoretical isotherms. The removal efficiency of ALHUM was above 75% indicating that the ALHUM can be used as efficient adsorbent for cationic dye removal and for clean and ecofriendly processes.

Keywords: Alumina; Humic acid; Organic dyes; Adsorption

1. Introduction

Organic dyes are widely used in textile, tanning the leather, paper, plastic and other industries [1–4]. These substances are divided into three categories: (i) anionic (acids dyes), (ii) cationic (basic dyes) and (iii) non-ionic (disperse dyes) dyes, and they represent one of the problematic pollutants in wastewater [5,6]. Dyes which usually have a synthetic origin are generally characterized by complex aromatic molecular structures which resist to environmental conditions such as light and microbial attack [7]. Most dyes have toxic as well as carcinogenic, mutagenic and teratogenic effects [8], on environment and also on humans and animals health [9,10]. At higher concentration, the methylene blue (MB) dye is an example of dyes causing enormous damage to humans and animals health

---

* Corresponding author.

Presented at the 5th International Conference on Sustainable Solid Waste Management (ATHENS 2017), 21–24 June 2017, Athens, Greece.

such as eyes burns, respiratory problems, nausea, vomiting, profuse sweating and mental confusion [11]. In order to preserve the human's health and environment, notably hydrosphere, the treatment of effluent containing such dye is of great concern.

Removal techniques of dyes may be included in three categories: physical, chemical and biological [12]. However, biological wastewater treatment processes were found to be ineffective in the removal of the dyes [13,14] because of their low biodegradability [15]. Among the physical methods available, adsorption process has proven to be effective in the removal of colour from wastewater, and it is one of the powerful and low cost treatment processes [16]. Many adsorbents are used to reduce dye concentration from aqueous solutions. Activated carbon is regarded as an effective but expensive adsorbent due to its high cost of manufacturing and regeneration [17]. Hence, there is a need for an effective and cheaper material as an alternative adsorbent for removing the dyes from water. Hence, some natural adsorbents including quartz [18], kaolinite [19], montmorillonite modified with chitosan [20], clay minerals, and some natural biomass and polymeric resin have also been reported [21,22]. For these natural adsorbent, a considerable amount of work has been reported in the literature, regarding the adsorption of some dyes on their surfaces. However, very few studies have dealt with the use of oxides minerals modified with humic acid (HA) as natural adsorbent for dyes removal from water. Indeed, in natural environment, most inorganic particles surfaces are coated with adsorbed natural organic matter such as humic substance [23]. Such organic coatings are known to alter the surface charge and aggregation behaviour of mineral particles. The aim of the present study is to assess the potentiality of oxide aluminium (alumina) modified with HA as adsorbent for the removal of MB dye from aqueous solution. For this purpose, humic-coated alumina (ALHUM) particles were first prepared and characterized. Thereafter, adsorption kinetics and isotherms were investigated as a function of contact time, pH, ionic strength, temperature and the nature of divalent cations present in the aqueous solution. Finally, the equilibrium data were analyzed using Langmuir, Freundlich and Dubinin–Radushkevich isotherm models.

2. Experimental

2.1. Materials

2.1.1. Cationic dye

The MB used in this study was purchased from Merck. The properties of MB are given in Table 1.

The chemical structure of dye is given in Fig. 1.

2.1.2. Humic acid

The HA used in the study (sodium humate) was purchased from Aldrich-Chimie (France). It was used as-received without further purification. Characteristics of HA, such as its molecular weight, which is around 2,000 g/mol, and its elemental analysis which gives C (38.02%), H (3.76%), N (0.52%), O (57.4%) and S (<0.3%), were described elsewhere [24].

Table 1
Selected physical and chemical characteristics of methylene blue (MB)

Compound	Methylene blue
Class	Thiazin
Chemical formula	$C_{16}H_{18}N_3ClS$
C.I. name	Basic blue
Molecular weight (g/mol)	319.86
Water solubility (g/L)	50 (20°C)

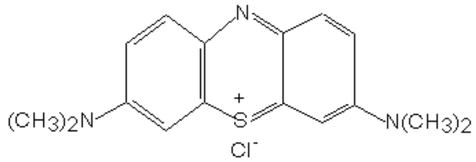

Fig. 1. Chemical structure of methylene blue.

2.1.3. Alumina

Commercial oxide aluminium Al_2O_3 (alumina) mineral particles was supplied by Merck (Morocco), and used without further purification. The zeta potential measurements of alumina have shown that the point of zero charge (pH_{PZC}) is about 9 [25].

2.2. Reagents

All chemical reagents employed in this work were puriss p.a., ACS reagent, and the aqueous solutions were prepared using all instances by distilled water. The ionic strength was fixed by using sodium chloride (NaCl) as salt. The pH of the solution was adjusted to the desired values by using solutions of HCl or NaOH (0.1 M). Aqueous solutions of calcium chloride ($CaCl_2$), copper chloride ($CuCl_2$) and barium chloride ($BaCl_2$) were prepared and used to study the nature's effect of divalent cation on adsorption of MB onto humic-covered alumina (ALHUM).

2.3. Preparation of humic coated-alumina

For the preparation of HA coated alumina, 50 mg of alumina was placed in stoppered bottle and 50 mL of NaCl 10^{-2} M containing 50 mg/L of HA was added. The pHs suspension was adjusted to 5 and agitated at 20°C for 24 h, then centrifuged at ambient temperature for 30 min at 4,000 rpm to settle HA-covered alumina particles. These particles were dried at 40°C for 12 h. The coating HA-covered alumina formed is characterized by different techniques.

2.4. Solid characterization

The solid samples (the simple alumina and the HA-coated alumina) were analyzed by scanning electron microscopic (SEM) in order to get further insight into HA-coated alumina structure and morphology. The particles surface charges were assessed by titration of the solid samples with aqueous cationic surfactant solutions made of cetyltrimethylammonium chloride (CTACL), and by using a potential measuring device (particle charge detection, PCD, Müteck Instrument), as described elsewhere [24].

2.5. Adsorption experiments

To study the effects of various parameters (pH, ionic strength, temperature and nature of divalent cation) on the adsorption of MB dye onto ALHUM, various series of ALHUM-dye aqueous dispersions were prepared. An aqueous MB solution with a concentration of 1 g/L was prepared as stock solution, being used for preparing the rest of the solutions by dilution.

All adsorption tests were carried out in stoppered bottles immersed in a thermostatic bath at a constant agitation speed.

The kinetic study was carried out by adding amount of 60 mg of HA-coated alumina into 60 mL of dye solutions with a concentration of 50 mg/L at pH = 6 and 10^{-2} M of NaCl. The mixtures were placed under a constant agitation time ranging from 10 to 500 nm.

In the subsequent series dealing with the effects of pH, ionic strength and nature of divalent cation, a weighed amount of ALHUM solid (60 mg) was placed in stoppered bottles and known volumes (60 mL) of salt solutions (monovalent or divalent cation) aqueous solutions containing various amounts of dye (initial dye concentration, C_{initial}, ranging from 10 to 150 mg/L) were added. The effect of pH was investigated by adjusting the dyes – HA-coated alumina aqueous dispersions to desired pH values (pH = 4, 6, 8 and 10) in 10^{-2} M of NaCl solution.

To study the effect of ionic strength, dispersion containing various NaCl concentrations (10^{-3} to 10^{-1} M) at pH 6 were prepared. The effect of divalent cation nature was studied by adding various salts ($CuCl_2$, $BaCl_2$ and $CaCl_2$) to the dispersions at fixed salt concentration of 10^{-2} M at pH = 6. The control of the temperature was carried out by a thermostatic bath regulated at temperatures ranging from 293 to 323 K. For this purpose, dispersions containing 60 mg of HA-coated alumina mixture with 50 mg/L of dye were prepared in 60 mL of NaCl salt (10^{-2} M). These dispersions were agitated for a contact time varying from 10 to 500 min.

Once the experiments were finished, the adsorbent was separated from the liquid phase by centrifugation at 4,000 rpm for 30 min. The residual concentration of the supernatant was measured by a spectrophotometer at 665 nm.

The adsorbed amount, Q_{ads}, as expressed in milligram of dye per gram of the solid, was determined from the difference between the initial concentration (C_{initial}) and the residual concentration ($C_{\text{equilibrium}}$), according to the equation:

$$Q = (C_{\text{initial}} - C_{\text{eq}})/m_s \tag{1}$$

where m_s is the amount of the ALHUM adsorbent (g/L), C_{initial} and C_{eq} are initial and residual dye concentrations, respectively (mg/L).

3. Theoretical

3.1. Adsorption isotherm

All adsorbent/adsorbate systems are not behaving the same way. The adsorption phenomena are often addressed by their isotherm behaviour. Isotherms describe the existing relationship between the adsorbed amount and the solute concentration at equilibrium and at constant temperature. These isotherms were studied using a several well-known isotherm models such as Langmuir, Freundlich and Dubinin–Radushkevich (D-R) models.

3.1.1. Langmuir model

Langmuir isotherm assumes that adsorption take place on a homogeneous adsorbent surface of identical sites that are equally available and energetically equivalent [26]. Further, this model is applicable to monolayer chemisorption [27].

The mathematical expression of Langmuir model, and its linearized form are given by Eqs. (2) and (3), respectively:

$$\frac{q_e}{q_{\max}} = \frac{k_L C_e}{1 + K_L C_e} \tag{2}$$

$$\frac{1}{q_e} = \frac{1}{C_e} \times \frac{1}{q_{\max} K_L} + \frac{1}{q_{\max}} \tag{3}$$

where q_e is the amount of solute adsorbed per links of adsorbent (mg/g); C_e is the concentration of solute remaining in solution at equilibrium (g/L); C_{eq} is the equilibrium dye concentration in aqueous phase (mg/L), K_L is the Langmuir equilibrium constant (L/mg) and q_m is the maximum adsorption capacity (mg/g).

3.1.2. Freundlich model

Freundlich isotherm is widely used to describe adsorption on a surface having heterogeneous energy distribution. This energy varies as a function of surface coverage [28]. A mathematical expression of the Freundlich model is:

$$q_e = K_F \times C_e^n \tag{4}$$

$$\log q_e = \log K_F + n \log C_e \tag{5}$$

where K_F and n are Freundlich constants. One of the Freundlich constants K_F indicates the adsorption capacity of the adsorbent. The other Freundlich constant n is a measure of the deviation from linearity of the adsorption. The magnitude of the exponent n values will indicate if the adsorption is favourable or not. Thus, a value of $n > 1$ indicates a favourable adsorption. However, when n is between 0 and 1, the adsorption is unfavourable [11].

3.1.3. Dubinin–Radushkevich model

The Dubinin–Radushkevich isotherm model assumes that the adsorption potential is variable and that the free enthalpy of adsorption is related to the pore filling degree, unlike the Langmuir model [29]. The D-R expression is represented by the following equations:

$$q_e = q_m e^{-\beta \varepsilon^2} \tag{6}$$

$$\varepsilon^2 = RT\ln\left(1+\frac{1}{C_e}\right) \tag{7}$$

where q_m is the maximum adsorption capacity (mg/g), ε is the Polanyi potential, β is a constant related to the adsorption energy, E (kJ/mg), by the following equation:

$$E = \frac{1}{\beta^{0.5}} \tag{8}$$

The linear form of Dubinin–Radushkevich model is:

$$\ln q_e = \ln q_m - \beta RT\ln\left(1+\frac{1}{C_e}\right) \tag{9}$$

3.2. Kinetics of adsorption

In order to gain a better understanding of the kinetics and the rate determining step of adsorption processes, the pseudo-first-order [30], the pseudo-second-order [31] and the intra-particle diffusion models [32] were employed.

- The pseudo-first-order model is given by equation:

$$\frac{dq(t)}{dt} = K_1(q_e - q(t)) \tag{10a}$$

where $q(t)$ and q_e are respectively the amounts adsorbed per unit mass of the adsorbent (both in mg/g) at any time and at equilibrium, and K_1 is the pseudo-first-order rate constant of adsorption (min^{-1}). The linearized form of Eq. (10a) is expressed by the following equation:

$$\ln(q_e - q_t) = \ln q_e - K_1(t) \tag{10b}$$

- The pseudo-second-order model is expressed as:

$$\frac{dq(t)}{dt} = K_2(q_e - q(t))^2 \tag{11a}$$

where K_2 is the rate constant of pseudo-second-order adsorption. Integration of this Eq. (11a) gives Eq. (11b):

$$q(t) = \frac{K_2 q_e{}^2 t}{1 + K_2 q_e t} \tag{11b}$$

- Intra-particle diffusion model:

The transfer of the solute from the aqueous phase to the surface of the adsorbent involves multistep such as external diffusion and internal diffusion, pore diffusion, surface diffusion and adsorption into the pore surface. The intra-particle diffusion model used to study the diffusion in adsorption system is originated from Fick's second law and is written as [33,34]:

$$q(t) = K_i t^{0.5} + \text{Cste} \tag{12}$$

where K_i is the intra-particle diffusion rate constant (mg/g min$^{0.5}$) and Cste (mg/g) is a constant.

4. Results and discussion

4.1. Characterization of the HA-coated alumina

The isoelectrical point (IEP) of the solid samples (the natural Al_2O_3 particles, and the HA covered Al_2O_3 particles) were evaluated by titration of the solid aqueous dispersions with CTACL which is a cationic surfactant, and using a potential measuring device (PCD, Müteck Instrument). Fig. 2 shows the titration curves of the natural and the HA covered Al_2O_3 particles, by CTACL.

As can be seen in Fig. 2, the adsorption of HA onto alumina particles, leads to a significant reduction of the solid's IEP from 8.025×10^{-8} mmol of CTACL for the natural alumina, to 4.900×10^{-8} mmol of CTACL for the HA covered alumina, that is, a solid IEP decrease of about 61%. Such solid sample IEP decrease results from the solid surface charge decrease which is due to the screening of the alumina surface charge by HA particles.

Fig. 3 shows the SEM pictures of the natural and the HA covered alumina particles. As can be seen in this figure, the HA adsorption from water onto alumina particles leads to an increase in the solid particle size, as resulting from the

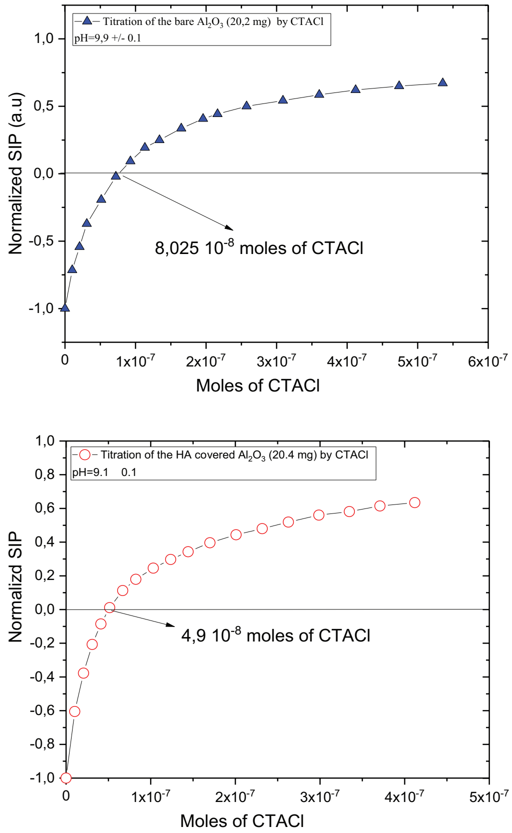

Fig. 2. Titration curves of the natural Al_2O_3 particles (top), and the humic acid covered Al_2O_3 particles (bottom), by CTACL ([solid] = 2 g/L, temperature $T = 20°$).

solid surface charge screening and/or flocculation of alumina particles by HA.

4.2. Effect of humic acid on adsorption of MB dye by alumina

To investigate the influence of HA on adsorption of MB dye, a series of adsorption experiments of dye on simple alumina alone and alumina modified by different HA concentrations (50 and 100 mg/L) was carried out at ambient temperature (T = 20°C). The adsorption isotherms of MB by alumina are shown in Fig. 4. As can be seen, the presence of HA coated to alumina, exhibited a rather pronounced effect on the adsorption of MB. Consequently, coating alumina surface with a large amount of HA improves the removal of MB from aqueous solution. Indeed, the adsorption of HA on surface of alumina causes modification of surface charge; this latter would become negative. This promotes the attraction between the cationic dye (MB) and the alumina coated with HA (ALHUM) via electrostatic interaction. This result is consistent with the reported work of Almeida et al. [35]. These authors reported higher adsorption MB on montmorillonite clay has a negatively charged surface similar to that observed on ALHUM particles.

In another work, Zermane et al. [36] have found that HA affects favourably the adsorption of basic yellow 28 dye on iron oxides. This result explained by the fact that the adsorbent surface become more negative after the immobilization of HA and this promoted to adsorb positive charged cationic dye via electrostatic interaction by Vinod and Anirhudan [37].

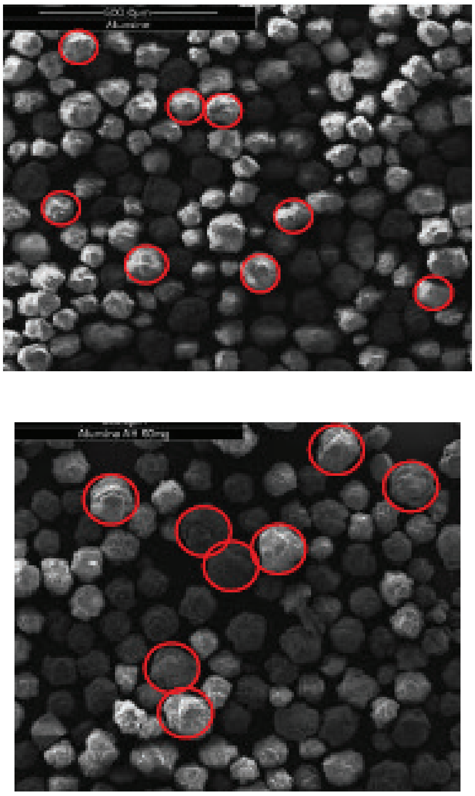

Fig. 3. SEM pictures of the natural Al_2O_3 particles (top) and the humic acid covered Al_2O_3 particles (bottom).

Other authors have shown that the presence of HA controls the mobility of cationic dyes in environment [38–40]. This effect was attributed to the binding between basic dyes and HA by different interactions types such as electrostatic, donor–acceptor and hydrophobic interactions [32].

In what follows, we will work with alumina particles mixed with 50 mg/L of HA (ALHUM).

4.3. Effect of contact time

In order to determine the required time to reach equilibrium, an adsorption experiment of MB at a fixed concentration on ALHUM as a function of contact time was studied. The result obtained is presented in Fig. 5. As can be in Fig. 5, the equilibrium adsorption of MB dye onto ALHUM is reached after 2 h of contact time. After this time, the adsorbed amount remains constant despite the increase in contact time. In addition, it is noted that almost 50% of dye has been removed in

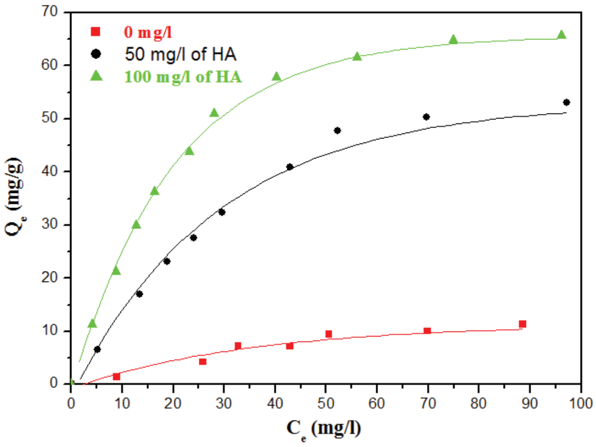

Fig. 4. Effect of amount of humic acid on adsorption of MB by alumina ([solid] = 1 g/L, $I = 10^{-2}$ M, pH = 6, ambient temperature, T = 20°C).

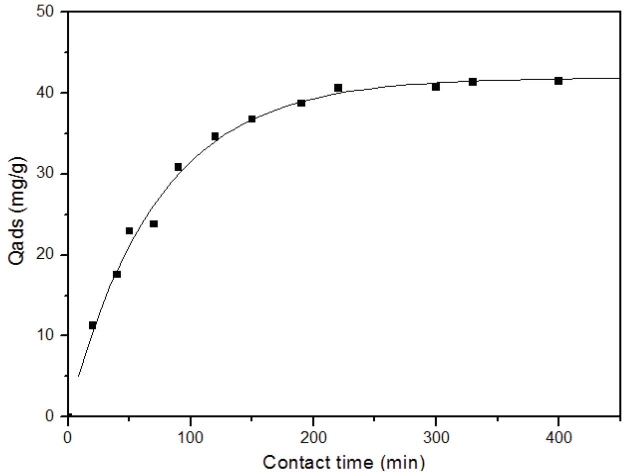

Fig. 5. Effect of contact time on the adsorption of MB onto HA-coated alumina solid ([MB] = 50 mg/L, pH = 6, [solid] = 1 g/L, $I = 10^{-2}$ M NaCl, ambient temperature, T = 20°C).

less than 50 min. However, in the remainder of the adsorption experiments, we will fix the contact time at 3 h.

The experimental kinetic data for MB adsorption on HA-coated alumina solid are fitted with the pseudo-first-order, the pseudo-second-order and the intra-particle diffusion models and presented in Figs. 6(A)–(C), respectively.

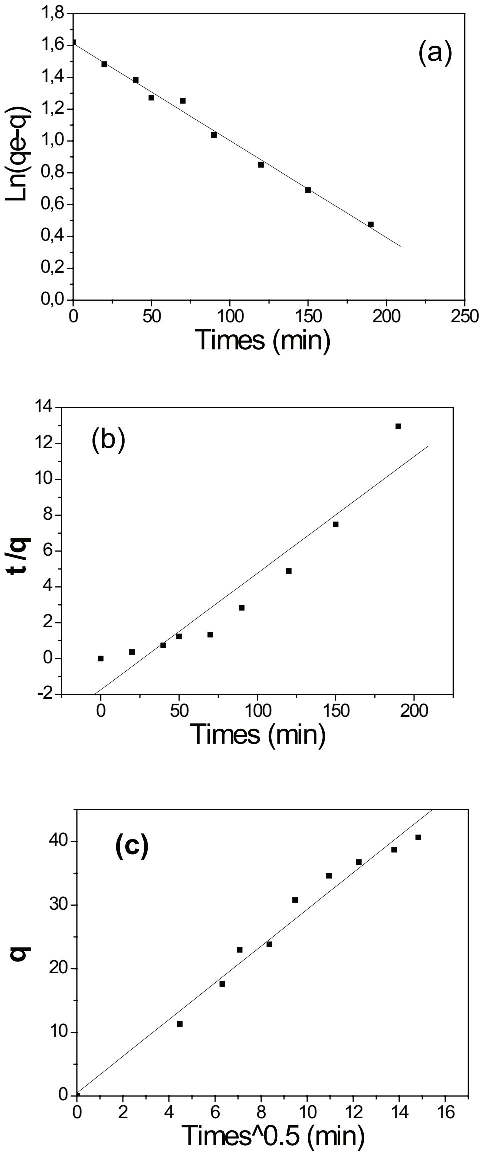

Fig. 6. (A) Pseudo-first-order kinetic plots for MB adsorption onto ALHUM, (B) pseudo-second-order kinetic plots for MB adsorption onto ALHUM and (C) intra-particle diffusion kinetic plots for MB adsorption onto ALHUM.

As shown in Fig. 6(A), the adsorption kinetics data fit the pseudo-first-order model very well. The correlation coefficient, *r*, was 0.996. Furthermore, the adsorption system of MB followed the intra-particle diffusion model, with the correlation coefficients, *r* value of 0.988. However, estimated adsorbed amount at equilibrium q_e is reasonably close to experimental q_e value in the case of pseudo-first-order model. The adsorption of MB can be fit by the pseudo-second-order kinetic equation, and the regression correlation coefficients, *r*, was 0.948. This result shows that the adsorption process of MB onto ALHUM particles may be controlled by the combined effect of surface adsorption and intra-particle diffusion.

This result is consistent with the reported work of Yan et al. [41]. These authors suggested that the adsorption rate of dyes onto organo-bentonite was dominated by similar effects such as surface adsorption, liquid diffusion process and internal surface adsorption. In another work, Zermane et al. [36] have reported that the adsorption rate of basic yellow 28 dye onto HA modified iron oxides are depicted properly by the pseudo-first-order kinetic model.

The kinetic constants, correlation coefficients and experimental q_e values obtained from the linear plots were recapitulated in Table 2.

In literature, several authors have reported that the MB adsorption on various adsorbents followed a pseudo-first-order kinetic model [27,42]. The values of the rate constant, K_1, of pseudo-first-order kinetic model obtained in the present work is almost identical to that found by Shawabkeh and Tutunji [43].

4.4. Effect of pH on the adsorption of dye

Fig. 7(A) shows the MB adsorption isotherms onto the HA-coating alumina particles at ambient temperature (T = 20°C) and at pH 4, 6, 8 and 10. It should be recalled that the aqueous phase pH of the adsorbent preparation is pH = 5, at this pH, HA is negatively charged but alumina is positively charged (IEP of Al_2O_3 is around pH = 9). Note that for this adsorbent prepared at pH = 5, no desorption of HA was observed at higher pH values. The curves in Fig. 7(A) indicate that the adsorption is strong at high pH. The MB adsorbed amount increases from 35 to 79 mg/g when the pH of the medium increases from 4 to 10. From these observations, it was suggested that the adsorption of MB is dependent on the properties of the adsorbent surface. Further, the percentage of dye removal efficiency increased from 39.2% to 74.42% as pH of dye aqueous solution increased from 4 to 10 (Fig. 7(B)). In addition, these behaviours can be attributed to electrostatic interaction occurring between the ALHUM surface groups charged negatively and the functional groups of dye molecule charged positively. However, at basic pH, the amplitude of ALHUM negative charge surface becomes very high with increasing pH of aqueous solution, because of the

Table 2
Kinetic constants of MB adsorption on HA-coating alumina

Pseudo-first-order			Pseudo-second-order			Intra-particle diffusion		
Q_e (mg/g)	K_1 (min^{-1})	*r*	Q_e (mg/g)	K_2 (g/mg min)	*r*	K_i (mg/g min$^{0.5}$)	Cste (mg/g)	*r*
41.05	0.014	0.996	41.69	1.55×10^{-3}	0.948	2.884	0.470	0.988

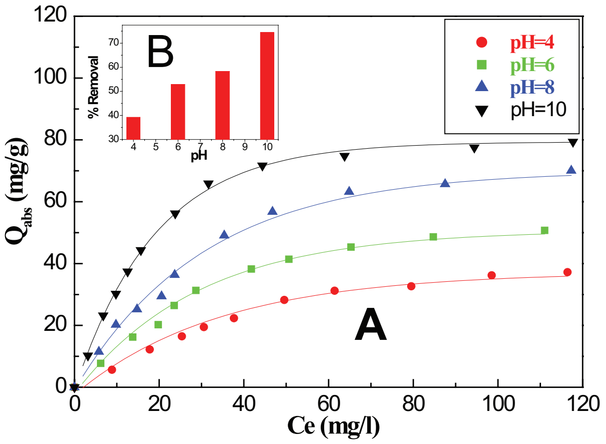

Fig. 7. Adsorption isotherms of MB onto HA-coated alumina particles (A) and percentages of dyes removal (B) at various pH values of the aqueous phase ([solid] = 1 g/L, $I = 10^{-2}$ M NaCl, ambient temperature, $T = 20°C$).

carboxylic groups of HA are ionized. In another study, Ait Akbour and Jada [44] have observed an increase of HA zeta potential magnitude, from –30 to –50 mV with increasing the pH value of the aqueous phase. These results were explained by the ionization of HA acidic groups, mainly carboxylic which occurs in the pH ranging from 3 to 10. Our results are in a good agreement with similar effects previously reported for adsorption of textile dyes by natural clays [45], and by Umpuch and Sakaew [20] for adsorption of methyl orange by chitosan intercalated montmorillonite.

Other authors have been studied the effect of pH on the adsorption of cationic dyes on organoclay [46]. They have shown that increasing the pH of the aqueous solution improves the cationic dyes percentage removal via electrostatic attraction [47].

4.5. Effect of ionic strength

It should be noted that anionic dyes, such as reactive dyes are usually used in the dying process of cellulosic fibres, which are the most prevalent textile fibres. Since the cellulosic fibre and the dye are negatively charged, repulsion occurs leading to reduction in the fibre staining. To overcome this problem, NaCl or other salt is added during the dying process to reduce the repulsion occurring between the fibre and the anionic dye and to enhance the fibre staining. Therefore, due to the important influence of ionic strength in the adsorption process [48], the effect of NaCl concentration on the MB adsorption capacity from aqueous solution onto HA-coating alumina was examined. The amount of MB adsorbed on the ALHUM particles as a function of ionic strength is presented in Fig. 8.

It is found that MB adsorption onto ALHUM particles increases by lowering the ionic strength. In fact, significant decrease of the amount adsorbed from 61.33 to 35.50 mg/g as the ionic strength increases from 10^{-3} to 10^{-1} M. This result is similar to earlier finding for the adsorption of organic cation (MB) on quartz sand solid bearing negative surface charge as to this found on HA-coating alumina particles [18]. Thus in the present work, the presence of NaCl in the aqueous phase may affect the electrostatic interaction that occurs between the negatively charged ALHUM surface and the basic dye (MB). The data indicate that increasing the inorganic cation concentration (Na^+) in the solution competes with the organic cation (MB) to be adsorbed on ALHUM surface. Therefore, it is expected that the adsorbed MB amount should decrease with an increase of NaCl concentration.

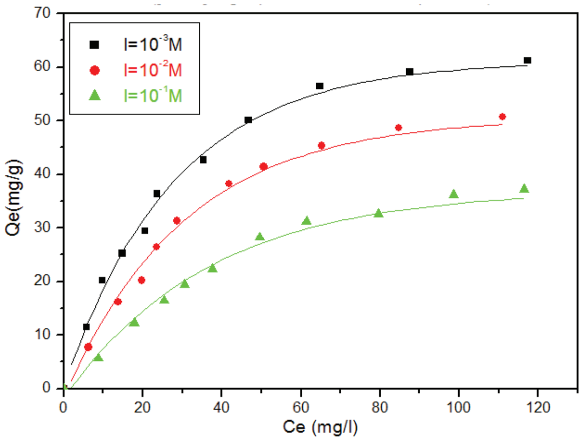

Fig. 8. Adsorption isotherms of MB onto HA-coated alumina particles at various ionic strength of the aqueous phase ([solid] = 1 g/L, pH = 6, ambient temperature, $T = 20°C$).

On the other hand, increasing ionic strength will promote aggregation, resulting in less specific surface, and then less dye removal.

Our results are in good agreement with similar effects previously reported for adsorption of astrazon red violet onto the montmorillonite [49]. These authors have found a decrease in the adsorption capacity with increasing the NaCl concentration. This result is explained by the presence of Na^+ ions at the montmorillonite surface which screen the electrostatic interactions between charges, consequently leading to less removal efficiency [50,51]. The increase of the positive ions fixing the ionic strength in solution has the effect of masking the negatively charged adsorbent surface, causing to the reduction of electrostatic interaction which leads to decrease of the cationic dye adsorption [47].

4.6. Effect of the nature of the divalent cation

In this experiment series, we examined the effect of divalent metal ion on the adsorption isotherms of MB dye from water onto HA-coating alumina solid. The divalent cations used were in the form of chloride salts ($CaCl_2$, $BaCl_2$ and $CuCl_2$) at a fixed concentration 10^{-2} M. The obtained data are presented in Fig. 9(A), and indicate that the adsorption capacity of MB is a function and dependent on the nature of divalent cation present in solution.

As it seen from Fig. 9(B), the MB adsorbed amount decreases in the sequence: $Cu^{2+} > Ba^{2+} > Ca^{2+}$. This behaviour may be explained by the cation affinity toward the ALHUM surface. Thus, the presence of divalent cation in the solution modifies and reduces the surface negative charge of the HA-coating alumina, resulting in reduction of the electrostatic attraction between the basic dye (MB) and the solid surface. It has been shown that the divalent cation Cu^{2+} form

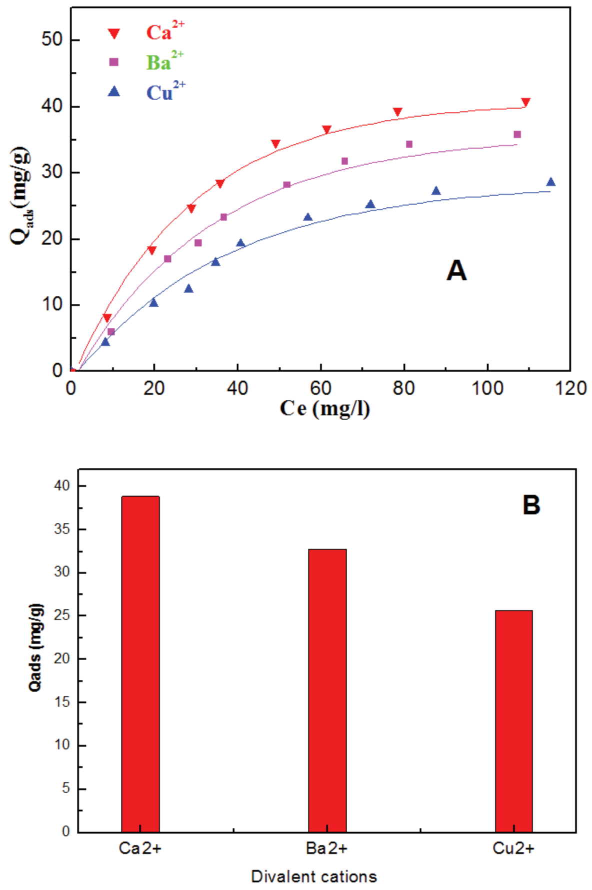

Fig. 9. (A) Adsorption isotherms of MB onto HA-coated particles in the presence of various divalent cations ([solid] = 1 g/L, pH = 6, $[Me^{2+}] = 10^{-2}$ M). (B) MB adsorbed amount as a function of various divalent cation.

coordination complexes with the HA negatively charged groups and is more efficient than Ba^{2+} and Ca^{2+} in reducing the HA charge [24,44]. In fact, the adsorption of divalent cations such as Cu^{2+}, Ba^{2+} and Ca^{2+} from bulk water onto the HA-coating alumina surface reduce the thickness of ALHUM colloids electrical double layer and/or the zeta potential [52]. Thus, the low adsorption of MB on HA-coating alumina particles in the presence of Cu^{2+} is attributed to strong reduction of the number of negative sites on the solid surface. This behaviour is consistent with the reported work of Ait Akbour and Jada [44]. These authors have found that the order of divalent cation complexing capacity and affinity toward HA macromolecules decrease in the sequence $Cu^{2+} > Ba^{2+} > Ca^{2+}$.

However, the higher MB adsorbed amount observed in the presence of Ca^{2+} as compared with Ba^{2+} or Cu^{2+} is likely due to the weak adsorption of the Ca^{2+} on the HA-coating alumina surface resulting a low reduction of the global negative charge of ALHUM particles.

4.7. Effect of temperature

Fig. 10(A) shows the variation of MB adsorption on ALHUM particles, vs. contact times, at 20°C, 30°C, 40°C and 50°C and at fixed pH and ionic strength values (pH = 6 and [NaCl] = 10^{-2} M). The amount of MB adsorbed on ALHUM solid as a function of temperature is presented in Table 2. The obtained data indicate a slight increase in the adsorption capacity of MB basic dye, from 25.17 to around 30.73 mg/g, when increasing the solution temperature values from 20°C to 50°C. Further, as can be seen in Fig. 10(B), the increase of solution temperature causes increase of the removal percentage of MB dye from aqueous phase.

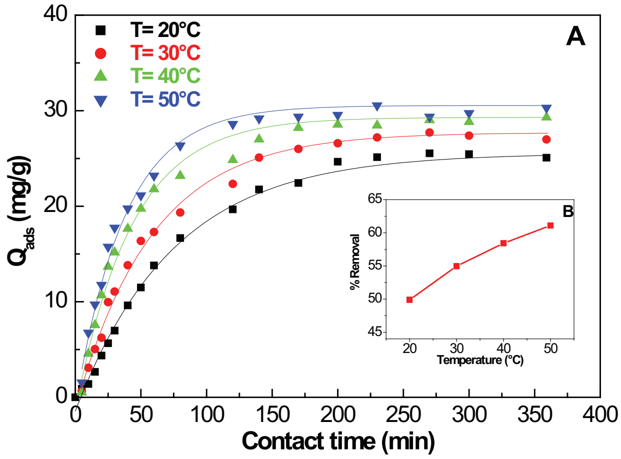

Fig. 10. Adsorption of MB onto HA-coated alumina solid (A), and percentages of dyes removal at various temperature (B) ([solid] = 1 g/L, [MB] = 50 mg/L, pH = 6, $I = 10^{-2}$ M NaCl).

This behaviour proves that the adsorption of MB at HA-coating alumina/aqueous solution interface is an endothermic process. This result indicated an increase in feasibility of adsorption at higher temperature. Thus, the increase in the MB adsorbed amount with increasing temperature can be explained by the combination of two phenomena: (i) the strong adsorptive forces between the actives sites of ALHUM particles and MB molecule and (ii) a strong thermal agitation resulting higher diffusion of MB molecules from the aqueous phase to ALHUM particles surface. Several authors have observed same effect of temperature on dye molecules adsorption [53–55].

Several authors have been reported that the adsorption of dyes on different adsorbent increases with temperature, which indicates that the adsorption is endothermic process [47,56,57]. These authors concluded that the temperature affect hugely adsorption processes [46,58]. Recently, Wang et al. [59] have also found that the adsorption of anionic azo dyes on surfactant modified flax shives was endothermic.

The thermodynamic parameters for adsorption of MB dye onto ALHUM were given by the following equation:

$$\Delta G° = -RT\ln(K_0) \quad (13)$$

where $\Delta G°$ is the standard free energy change (J/mol), R is the gas constant (8.314 J/mol K), T is the absolute temperature (K) and K_0 is the equilibrium constant given by equation:

$$\ln(K_0) = -\Delta H°/RT + \Delta S°/R \quad (14)$$

$\Delta H°$ and $\Delta S°$ are the enthalpy and entropy of adsorption reaction, respectively. The values of $\Delta H°$ and $\Delta S°$ can be obtained from the intercept and slope of the plot of ln(K) against 1/T. The values of ΔH° and ΔS° concluded from Eq. (14) and given in Table 3. As shown in Table 3, the free energy values are negatives and vary from –188.44 to –1,245.44 J/mol when the temperature increases from 298 to 323 K. The negative values of ΔG° indicate that the adsorption process is a spontaneous reaction. It is also noted that the ΔH° and ΔS° values are 12.411 kJ/mol and 42.28 J/K mol, respectively. The positive values of enthalpy change confirm that the adsorption of MB dye onto ALHUM is endothermic process, which implies that the adsorption is favourable with the increase of temperature. The positive values of ΔS° reflect an increase in randomness at the solid–solution interface during the adsorption of dye [60]. The same trend was reported by Huang et al. [61] in the study of the adsorption of organic pollutants of dye wastewater onto modified bentonite.

4.8. Adsorption modelling

The adsorption isotherms of MB basic dye onto HA-coating alumina at different experimental conditions were fitted with as Langmuir, Freundlich and Dubinin–Radushkevich models, Eqs. (3), (5) and (6). The maximum adsorption capacity, the model constant values and the correlation coefficient are presented in Table 4.

Where $q_{\max}$ is the maximum adsorption capacity (mg/g), K_L is the Langmuir equilibrium constant (L/mg), K_F is the Freundlich constant (mg$^{1-1/n}$/L$^{1/n}$/g), β is the constant related to the adsorption energy (mol/J), n is the heterogeneity factor and r is the correlation coefficient.

Table 3
Thermodynamic parameters from the adsorption of MB dye by HA-coating alumina

T (K)	Q_{ads} (mg/g)	K_D (L/g)	ΔG° (J/mol)	ΔH° (kJ/mol)	ΔS° (J/K mol)
298	24.58	–0.033	–188.44	12.411	42.28
303	27.38	0.190	–399.84		
313	29.11	0.331	–822.64		
323	30.45	0.443	–1,245.44		

The parameters appearing in equation for each model were determined by non-linear regression analysis. The calculated constants of the three isotherm equations are given in Table 4. The regression correlation coefficient (r) is also presented in Table 4. This table shows that for Langmuir isotherm, the values of correlation coefficients, r, were above 0.990 at different experimental conditions. On the other hand, a large difference between the experimental and calculated, q_e, values have been found. This result suggests that the adsorption process of MB on ALHUM particles was not monolayer adsorption.

For Freundlich isotherm model, the value reached for the regression correlation coefficient, r, is 0.980, and the values of n are less than 1. These results indicate that the MB adsorption onto ALHUM is not favourable under experimental conditions used in this study.

However, the Dubinin–Radushkevich model is found to better represent the experimental data with a value of the regression correlation coefficient, r, of 0.995, and the calculated q_e value obtained from this model is in good agreement with experimental q_e value. The Dubinin model is usually used to calculate the energy of the adsorption process, as mentioned in Eqs. (6)–(9). In the present work (Table 4), we have used this model to determine the constant β, which is related to the adsorption energy ($E = 1/\beta^{0.5}$) of the dye on the solid surface. The data in Table 4 indicate that, as expected, the adsorption energy increases with the increase of the adsorbed maximum amount $q_{\max}$. Further, the data reveal heterogeneous surface adsorption of MB on HA covered alumina solid. The Dubinin–Radushkevich model is better for modelling the adsorption of MB dyes on the ALHUM particles. A similar result was found by Elmoubarki et al. [45] for the adsorption of textile dyes on raw Moroccan clays.

5. Conclusions

This study investigated the adsorption characteristics and the suitability of HA covered alumina (ALHUM) as potential adsorbent for the removal of MB from aqueous solutions and by using batch mode. The results reveal that the adsorption was dependent on various parameters such as the aqueous phase pH, the ionic strength,

Table 4
Isotherm models constants for MB adsorption onto HA-coating alumina

		Langmuir			Freundlich			D-R		
		$q_{\max}$	K_L	r	K_F	n	r	$q_{\max}$	β	r
pH	4	114.4	6.1×10^{-3}	0.994	1.5	0.71	0.973	40.2	3.41×10^{-3}	0.988
	6	100.3	1.4×10^{-2}	0.997	2.9	0.66	0.971	51.3	3.47×10^{-3}	0.992
	8	105.9	2.2×10^{-2}	0.995	4.9	0.60	0.976	68.3	2.13×10^{-3}	0.989
	10	142.2	2.5×10^{-2}	0.994	6.2	0.66	0.969	78.9	1.40×10^{-3}	0.994
I (M)	10^{-1}	114.4	6.1×10^{-3}	0.994	1.5	0.71	0.973	40.2	3.41×10^{-3}	0.988
	10^{-2}	100.3	1.4×10^{-2}	0.997	2.9	0.66	0.971	51.3	3.47×10^{-3}	0.992
	10^{-3}	88.2	2.7×10^{-2}	0.995	5.6	0.54	0.972	60.9	1.96×10^{-3}	0.988
Me^{2+}	Ca^{2+}	87.6	1.2×10^{-2}	0.995	5.1	0.46	0.962	46.0	2.82×10^{-3}	0.993
	Ba^{2+}	157.7	4.2×10^{-3}	0.990	3.5	0.52	0.981	41.4	3.52×10^{-3}	0.995
	Cu^{2+}	68.9	8.3×10^{-3}	0.997	1.8	0.61	0.969	29.6	3.10×10^{-3}	0.988

the temperature and the nature of the divalent cation. Thus, the MB adsorbed amount onto the ALHUM was found to increase by increasing either the aqueous phase pH or the temperature of the adsorption medium. However, decreases in the MB adsorbed amount were observed upon the increase of the divalent cation (Ca^{2+}, Ba^{2+} and Cu^{2+}) affinity toward the ALHUM and/or the aqueous solution ionic strength. The adsorption isotherms were well fitted by the Dubinin–Radushkevich adsorption model, and followed the pseudo-first-order kinetic model.

Finally, the overall data suggested that ALHUM is a potential adsorbent for the reduction of dye accumulations normally found in various industrial effluents.

Acknowledgements

The financial supports by the European ERANET MED Water-13_043 (Project SETPROpER: Sustainable treatment processes of effluents for reuse of water in agriculture) and CNRST-Maroc are gratefully acknowledged.

Symbols

R — Gas constant
T — Temperature
t — Contact time adsorbate–adsorbent
$q(t)$ — Amount of adsorbate in the adsorbent at any time t
q_e — Amount of adsorbate in the adsorbent at equilibrium
Q, Q_{ads} — Adsorbed amount of the solute (the dye) on the solid surface
C_{initial} — Initial concentration of the solute (the dye)
C_e, C_{eq} — Residual concentration of the solute (the dye)
Cste — Constant
m_s — Amount of the adsorbent solid
$q_{\max}$, q_m — Maximum adsorption capacity
K_L — Langmuir equilibrium constant
K_F — Freundlich constant
K_1 — Pseudo-first-order rate constant of adsorption
K_2 — Pseudo-second-order rate constant of adsorption
K_i — Particle diffusion constant
n — Freundlich constant
E — Adsorption energy
β — Constant related to the adsorption energy
ε — Polanyi potential

References

[1] A. Mohammadi, H. Daemi, M. Barikani, Fast removal of malachite green dye using novel superparamagnetic sodium alginate-coated Fe_3O_4 nanoparticles, Int. J. Biol. Macromol., 69 (2014) 447–455.

[2] X. Ren, X. Zhang, L. Zhang, R. Han, Biosorption of methylene blue by natural and chemical modified wheat straw in fixed-bed column, Desal. Wat. Treat., 51 (2013) 4514–4523.

[3] M. Roosta, M. Ghaedi, A. Daneshfar, R. Sahraei, A. Asghari, Optimization of the ultrasonic assisted removal of methylene blue by gold nanoparticles loaded on activated carbon using experimental design methodology, Ultrason. Sonochem., 21 (2014) 242–252.

[4] F.C. Wu, R.L. Tseng, High adsorption capacity NaOH-activated carbon for dye removal from aqueous solution, J. Hazard. Mater., 152 (2008) 1256–1267.

[5] S.P. Patil, B. Bethi, G.H. Sonawane, V.S. Shrivastava, S. Sonawane, Efficient adsorption and photocatalytic degradation of Rhodamine B dye over Bi_2O_3-bentonite nanocomposites: a kinetic study, J. Ind. Eng. Chem., 34 (2016) 356–363.

[6] C.D. Raman, S. Kanmani, Textile dye degradation using nano zero valent iron: a review, J. Environ. Manage., 177 (2016) 341–355.

[7] M. Dogan, M. Alkan, O. Demirbas, Y. Ozdemir, C. Ozmetin, Adsorption kinetics of maxilon blue GRL onto sepiolite from aqueous solutions, Chem. Eng. J., 124 (2006) 89–101.

[8] G. McKay, M.S. Otterburn, D.A. Aga, Fullers earth and fired clay as adsorbent for dye stuffs, equilibrium and rate constants, Water Air Soil Pollut., 24 (1985) 307–322.

[9] A.R. Gregory, S. Elliot, P. Kluge, Ames testing of direct black 3B parallel carcinogenecity, J. Appl. Toxicol., 1 (1991) 308–313.

[10] X. Han, W. Wang, X. Ma, Adsorption characteristics of methylene blue onto low cost biomass material lotus leaf, Chem. Eng. J., 171 (2011) 1–8.

[11] M.J. Ahmed, S.K. Dhedan, Equilibrium isotherms and kinetics modeling of methylene blue adsorption on agricultural wastes-based activated carbons, Fluid Phase Equilib., 317 (2012) 9–14.

[12] A. Latif, S. Noor, Q.M. Sharif, M. Najeebullah, Different techniques recently used for the treatment of textile dyeing effluents: a review, J. Chem. Soc. Pak., 32 (2010) 115–124.

[13] N. Kannan, M.M. Sundaram, Kinetics and mechanism of removal of methylene blue by adsorption on various carbons—a comparative study, J. Dyes Pigm., 51 (2001) 25–40.

[14] A.N. Fernandes, C.A.P. Almeida, C.T.B. Menezes, N.A. Debacher, M.M.D. Sierra, Removal of methylene blue from aqueous solution by peat, J. Hazard. Mater., 144 (2007) 412–419.

[15] S. Preethi, A. Sivasamy, S. Sivanesan, V. Ramamurthi, G. Swaminathan, Removal of safranin basic dye from aqueous solutions by adsorption onto corncob activated carbon, Ind. Eng. Chem. Res., 45 (2006) 7627–7632.

[16] L.R. Bonetto, F. Ferrarini, C. De Marco, J.S. Crespo, R. Guégan, M. Giovanela, Removal of methyl violet 2B dye from aqueous solution using a magnetic composite as an adsorbent, J. Water Process Eng., 6 (2015) 11–20.

[17] M.A. Ahmad, N.A. Ahmad Puad, O.S. Bello, Kinetic equilibrium and thermodynamic studies of synthetic dye removal using pomegranate peel activated carbon prepared by microwave-induced KOH activation, Water Resour. Ind., 6 (2014) 18–35.

[18] A. Jada, R. Ait Akbour, Transport of basic colorant through quartz sand, J. Colloid Sci. Biotechnol., 1 (2012) 1–7.

[19] K.O. Adebowale, B.I. Olu-Owalabi, E.C. Chigbundu, Removal of Safranin-O from aqueous solution by adsorption onto kaolinite clay, J. Encapsulation Adsorpt. Sci., 4 (2014) 89–104.

[20] Ch. Umpuch, S. Sakaew, Removal of methyl orange from aqueous solutions by adsorption using intercalated montmorillonite, Songklanakarin J. Sci. Technol., 35 (2013) 451–459.

[21] E.I. Unuabonah, A. Taubert, Clay-polymer nanocomposites (CPNs): adsorbents of the future for water treatment, Appl. Clay Sci., 99 (2014) 83–92.

[22] M.T. Yagub, T.K. Sen, S. Afroze, H.M. Ang, Dye and its removal from aqueous solution by adsorption. A review, Adv. Colloid Interface Sci., 209 (2014) 172–184.

[23] C.R. O'Melia, Aquatic Chemical Kinetics: Reactions Rates of Processes in Natural Waters, Werner Stumm, New York, 1990.

[24] A. Jada, R. Ait Akbour, J. Douch, Surface charge and adsorption from water onto quartz sand of humic acid, Chemosphere, 64 (2006) 1287–1295.

[25] S. Kumar, N. Rawat, A.S. Kar, B.S. Tomar, V.K. Manchanda, Effect of humic acid on sorption of technetium by alumina, J. Hazard. Mater., 192 (2011) 1040–1045.

[26] E.N. El Qada, S.J. Allen, G.M. Walker, Adsorption of Methylene Blue onto activated carbon produced from steam activated bituminous coal: a study of equilibrium adsorption isotherm, Chem. Eng. J., 124 (2006) 103–110.

[27] K.G. Bhattacharyya, A. Sharma, Kinetics and thermodynamics of Methylene Blue adsorption on Neem (*Azadirachta indica*) leaf powder, Dyes Pigm., 65 (2005) 51–59.

[28] H. Freundlich, W. Heller, The adsorption of cis- and trans-azobenzene, J. Am. Chem. Soc., 61 (1939) 2228–2230.

[29] M.M. Dubinin, L.V. Radushkevich, The equation of the characteristic curves of the activated charcoal, Proc. Acad. Sci. USSR, Phys. Chem. Sect., 55 (1947) 331–337.

[30] Y.S. Ho, Citation review of Lagergren kinetic rate equation on adsorption reactions, Sientometrics, 59 (2004) 171–177.

[31] Y.S. Ho, G. McKay, The kinetics of sorption of divalent metal ions onto sphagnum moss peat, Water Res., 34 (2000) 735–742.

[32] S. Tunali, A.S. Özcan, A. Özcan, T. Gedikbey, Kinetics and equilibrium studies for the adsorption of Acid Red 57 from aqueous solutions onto calcined-alunite, J. Hazard. Mater., 135 (2006) 141–148.

[33] Y.S. Ho, G. McKay, Sorption of dye from aqueous solution by pit, Chem. Eng. J., 70 (1998) 115–124.

[34] R.S. Juang, F.C. Wu, R.L. Tseng, Mechanism of adsorption of dyes and phenols from water using activated carbons prepared from plum kernels, J. Colloid Interface Sci., 227 (2000) 437–444.

[35] C.A.P. Almeida, N.A. Debacher, A.J. Downs, L. Cottet, C.A.D. Mello, Removal of methylene blue from colored effluent by adsorption on montmorillonite clay, J. Colloid Interface Sci., 332 (2009) 46–53.

[36] F. Zermane, B. Cheknane, J.Ph. Basly, O. Bouras, M. Baudu, Influence of humic acids on the adsorption of Basic Yellow 28 dye onto an iron organo–inorgano pillared clay and two Hydrous Ferric Oxides, J. Colloid Interface Sci., 395 (2013) 212–216.

[37] V.P. Vinod, T.S. Anirhudan, Adsorption behaviour of basic dyes on the humic acid immobilized pillared clay, Water Air Soil Pollut., 150 (2003) 193–217.

[38] M. Ishiguro, L.K. Koopal, Predictive model of cationic surfactant binding to humic substances, Colloids Surf., A, 379 (2011) 70–78.

[39] G.P. Zanini, M.J. Avena, S. Fiol, F. Arce, Effects of pH and electrolyte concentration on the binding between a humic acid and an oxazine dye, Chemosphere, 63 (2006) 430–439.

[40] G.P. Sheng, M.L. Zhang, H.Q. Yu, Quantification of the interactions between a cationic dye and humic substances in aqueous solutions, J. Colloid Interface Sci., 331 (2009) 15–20.

[41] L. Yan, L. Qin, H. Yu, S. Li, R. Shan, B. Du, Adsorption of acid dyes from aqueous solution by CTMAB modified bentonite: kinetic and isotherm modeling, J. Mol. Liq., 211 (2015) 1074–1081.

[42] K.S. Low, C.K. Lee, K.K. Tan, Biosorption of basic dyes by water hyacinth roots, Bioresour. Technol., 52 (1995) 79–83.

[43] R.A. Shawabkeh, M.F. Tutunji, Experimental study and modeling of basic dye sorption by diatomaceous clay, Appl. Clay Sci., 24 (2003) 111–120.

[44] R. Ait Akbour, A. Jada, Effects of solution chemistry on the fluorescence and electrophoretic behaviours of humic acid, Colloid Sci. Biotechnol., 2 (2013) 1–8.

[45] R. Elmoubarki, F.Z. Mahjoubi, H. Tounsadi, J. Moustadraf, M. Abdennouri, A. Zouhri, A. El Albani, N. Barka, Adsorption of textile dyes on raw and decanted Moroccan clays: kinetics, equilibrium and thermodynamics, J. Water Resour. Ind., 9 (2015) 16–29.

[46] T.S. Anirudhan, M. Ramachandran, Adsorptive removal of basic dyes from aqueous solutions by surfactant modified halloysite clay (organoclay): kinetic and competitive adsorption isotherm, Process Saf. Environ. Prot., 95 (2015) 215–225.

[47] T. Ngulub, J.R. Gumbo, V. Masindi, A. Maity, An update on synthetic dyes adsorption onto clay based minerals: a state-of-art review, J. Environ. Manage., 191 (2017) 35–57.

[48] T.S. Anirudhan, M. Ramachandran, Surfactant-modified bentonite as adsorbent for the removal of humic acid from wastewaters, Appl. Clay Sci., 35 (2007) 276–281.

[49] B.A. Fil, M.T. Yilmaz, S. Bayar, M.T. Elkoca, Investigation of adsorption of the dye stuff astrazon red violet 3rn (basic violet 16) on montmorillonite clay, Braz. J. Chem. Eng., 31 (2014) 171–182.

[50] M. Dogan, M.H. Karaoglu, M. Alkan, Adsorption kinetics of maxilon yellow 4GL and maxilon red GRL dyes on kaolinite, J. Hazard. Mater., 165 (2009) 1142–1151.

[51] C.H. Weng, Y.T. Lin, T.W. Tzeng, Removal of methylene blue from aqueous solution by adsorption onto pineapple leaf powder, J. Hazard. Mater., 170 (2009) 417–424.

[52] M. Elimelech, C.R. O'Melia, Effect of particle size on collision efficiency in the deposition of Brownian particles with electrostatic energy barriers, Langmuir, 6 (1990) 1153–1163.

[53] D. Ghosh, K.G. Bhattacharyya, Adsorption of methylene blue on kaolinite, Appl. Clay Sci., 20 (2002) 295–300.

[54] M. Dogan, M. Alkan, Adsorption kinetics of methyl violet onto perlite, Chemosphere, 50 (2003) 517–528.

[55] W.T. Tsai, Y.M. Chang, C.W. Lai, C.C. Lo, Adsorption of basic dyes in aqueous solution by clay adsorbent from regenerated bleaching earth, Appl. Clay Sci., 29 (2005) 149–154.

[56] S. Karaca, A. Gürses, M. Açikyildiz, M. Ejder Korucu, Adsorption of cationic dye from aqueous solutions by activated carbon, Microporous Mesoporous Mater., 115 (2008) 376–382.

[57] Y. Zhao, E. Abdullayev, A. Vasiliev, Y. Lvov, Halloysite nano tubule clay for efficient water purification, J. Colloid Interface Sci., 406 (2013) 121–129.

[58] K. Chinoune, K. Bentale, Z. Bouberka, A. Nadim, U. Maschke, Adsorption of reactive dyes from aqueous solution by dirty bentonite, Appl. Clay Sci., 123 (2016) 64–75.

[59] W. Wang, G. Huang, Ch. An, X. Xin, Y. Zhang, X. Liu, Transport behaviors of anionic azo dyes at interface between surfactant-modified flax shives and aqueous solution: synchrotron infrared and adsorption studies, Appl. Surf. Sci., 405 (2017) 119–128.

[60] J. Ma, Y. Jia, Y. Jing, Y. Yao, J. Sun, Kinetics and thermodynamics of methylene blue adsorption by cobalt-hectorite composite, Dyes Pigm., 93 (2012) 1441–1446.

[61] Z. Huang, Y. Li, W. Chen, J. Shi, N. Zhang, X. Wang, Z. Li, L. Gao, Y. Zhang, Modified bentonite adsorption of organic pollutants of dye wastewater, Mater. Chem. Phys., 202 (2017) 266–276.